All-coupling polaron optical response: Analytic approaches beyond the adiabatic approximation

S. N. Klimin,[*] J. Tempere,[†] and J. T. Devreese[‡]
TQC, Universiteit Antwerpen, Universiteitsplein 1, B-2610 Antwerpen, Belgium
(Received 29 May 2016; revised manuscript received 1 September 2016; published 22 September 2016)

In the present work, the problem of an all-coupling analytic description for the optical conductivity of the Fröhlich polaron is treated, with the goal being to bridge the gap in the validity range that exists between two complementary methods: on the one hand, the memory-function formalism and, on the other hand, the strong-coupling expansion based on the Franck-Condon picture for the polaron response. At intermediate coupling, both methods were found to fail as they do not reproduce diagrammatic quantum Monte Carlo results. To resolve this, we modify the memory-function formalism with respect to the Feynman-Hellwarth-Iddings-Platzman approach in order to take into account a nonquadratic interaction in a model system for the polaron. The strong-coupling expansion is extended beyond the adiabatic approximation by including in the treatment nonadiabatic transitions between excited polaron states. The polaron optical conductivity that we obtain at $T = 0$ by combining the two extended methods agrees well, both qualitatively and quantitatively, with the diagrammatic quantum Monte Carlo results in the whole available range of the electron-phonon coupling strength.

DOI: 10.1103/PhysRevB.94.125206

I. INTRODUCTION

The polaron, first proposed as a physical concept by Landau [1] in the context of electrons in polar crystals, has become a generic notion describing a particle interacting with a quantized bosonic field. The polaron problem has consequently been used for a long time as a testing ground for various analytic and numerical methods with applications in quantum statistical physics and quantum field theory. In condensed-matter physics, the polaron effect coming from the electron-phonon interaction is a necessary ingredient in the description of the dc mobility and the optical response in polar crystals (see Ref. [2]). Polaronic effects are manifest in many interesting systems, such as magnetic polarons [3], polarons in semiconducting polymers [4], and complex oxides [5,6], which are described in terms of the small-polaron theory [7]. *Large-polaron* theory has recently been stimulated by the possibility to study polaronic effects using highly tunable quantum gases: the physics of an impurity immersed in an atomic Bose-Einstein condensate [8] can be modeled on the basis of a Fröhlich Hamiltonian. Another recent development in large-polaron physics stems from the experimental advances in the determination of the band structure of highly polar oxides [9], relevant for superconductivity, where the optical response of complex oxides explicitly shows the large-polaron features [10,11].

Diagrammatic quantum Monte Carlo (DQMC) methods have been applied in recent years to numerically calculate the ground-state energy and the optical conductivity of the Fröhlich polaron [12,13]. Advances in computational techniques such as DQMC have inspired renewed study of the key problem in polaron theory—an *analytic* description of the polaron response. For the *small-polaron* optical conductivity, the all-coupling analytic theory has been successfully developed [14], showing good agreement with the numeric results of the DQMC. However, the optical response problem for a *large polaron* is not yet completely solved analytically. It should be noted that here we refer to "analytic" methods, which in fact can require massive computations (e.g., the Feynman variational method and the methods used in the present work), in order to distinguish them from the purely numerical methods, such as DQMC.

Asymptotically exact analytic solutions for the polaron optical conductivity have been obtained in the limits of weak [15–17] and strong coupling [18,19]. A first proposal for an all-coupling approximation for the polaron optical conductivity has been formulated in Ref. [20] [referred to below as Devreese–De Sitter–Goovaerts (DSG)], further developing the Feynman-Hellwarth-Iddings-Platzman (FHIP) theory [21] and using the Feynman variational approach [22]. However, in Ref. [20], it was already demonstrated that FHIP is inconsistent at large α with the Heisenberg uncertainty relations. This inconsistency is revealed in Ref. [20] through extremely narrow peaks of the optical conductivity at large α. Nevertheless, the peak positions for the polaron optical conductivity as obtained in Ref. [20] have been confirmed with high accuracy [19] by the DQMC calculation [13]. This inspired further attempts to develop analytical methods for the polaron optical response, especially at intermediate and strong coupling. Among these analytic methods, an extension of the DSG method has been proposed in Ref. [18], introducing an extended memory-function formalism with a relaxation time determined from the additional sum rule for the polaron optical conductivity. Alternatively, for the strong-coupling regime, the strong-coupling expansion (SCE) based on the Franck-Condon scheme for multiphonon optical conductivity has been developed in Refs. [18,19].

In the limit of small α, the optical conductivity derived within the memory-function formalism (both DSG and extended methods [18,20]) analytically tends to the asymptotically exact perturbation results of Refs. [15–17]. As seen

[*]On leave from Department of Theoretical Physics, State University of Moldova, MD-2009 Kishinev, Republic of Moldova.
[†]Present address: Lyman Laboratory of Physics, Harvard University, Cambridge, Massachusetts 02138, USA.
[‡]Present address: Technische Universiteit Eindhoven, P.O. Box 513, 5600 MB Eindhoven, The Netherlands.

from the comparison of the memory-function polaron optical conductivity with numerically accurate DQMC data [13,18], they agree well with each other for $\alpha \lessapprox 4$ (for DSG) and for $\alpha \lessapprox 6$ (the extended memory-function formalism). As written above, the conclusion that the memory-function formalism based on the Feynman polaron model failed at large α due to inconsistency with the Heisenberg uncertainty relations was already formulated in Ref. [20].

The alternative method, i.e., the strong-coupling expansion of Refs. [18,19], is based on the adiabatic approximation for electron-phonon states which is asymptotically exact in the strong-coupling limit. In summary, the memory-function formalism is well substantiated for small and intermediate values of α, and the strong-coupling expansion adequately describes the opposite limit of large α. Consequently, the extended memory-function formalism and the strong-coupling expansion are complementary to each other. The quantitative comparison of these two methods with each other and with DQMC performed in Ref. [18] shows that they only qualitatively agree with each other and with the DQMC data in the range of intermediate-coupling strengths ($6 \lessapprox \alpha \lessapprox 10$). On the one hand, the memory-function formalism explicitly disagrees with DQMC at large α. On the other hand, the strong-coupling expansion only qualitatively reproduces the shape of the optical conductivity and fails at intermediate α [18,19].

The main aim of the current paper is to *extend both the memory-function formalism and the strong-coupling expansion in order to bridge the gap that remains between their regions of validity*, such that the combination of both methods allows one to find analytical results in agreement with the numeric DQMC results at all coupling. In the present work, as in Ref. [19], the $T = 0$ case is considered. We have added the following elements in the theory, which lead to an overlapping of the areas of applicability for the two aforesaid analytic methods. For weak- and intermediate-coupling strengths, an extension of the Feynman variational principle and the memory-function method for a polaron with a nonquadratic trial action has been developed. As distinct from the memory-function formalism of Ref. [18], we do not use additional sum rules and relaxation times, and we perform the calculation *ab initio*. For intermediate- and strong-coupling strengths, the strong-coupling expansion of Ref. [19] is extended beyond the adiabatic approximation in the following way.

In the strong-coupling approximation for polaron optical conductivity [18,19], the matrix elements for the electron-phonon interaction between electron states with different energies are neglected. This is consistent with the adiabatic approximation, as described below in detail. The similar approach is well recognized in the theory of multiphonon transitions in deep centers [23,24]. In the present work, transitions between different excited polaron states due to the electron-phonon interaction are also taken into account. Because these transitions are beyond the adiabatic approximation, they are referred to as "nonadiabatic transitions." The incorporation of nonadiabatic transitions in the treatment leads to a substantial expansion of the range of validity for the strong-coupling expansion towards smaller α and to an overall improvement of its agreement with DQMC.

The paper is organized as follows. In Sec. II, we describe an all-coupling analytic description for the polaron optical conductivity within the extended memory-function formalism with a nonparabolic trial action and the nonadiabatic strong-coupling expansion. Section III contains the discussion of the obtained optical conductivity spectra and their comparison with results of other methods and with the DQMC data. The discussion is followed by conclusions, given in Sec. IV.

II. ANALYTIC METHODS FOR THE POLARON OPTICAL CONDUCTIVITY

A. Memory-function formalism with a nonparabolic trial action

To generalize the memory-function formalism, we start by extending Feynman's variational approach to translation-invariant non-Gaussian trial actions. The electron-phonon system is described by the Fröhlich Hamiltonian, using the Feynman units with $\hbar = 1$, the longitudinal-optical (LO) phonon frequency $\omega_{\mathrm{LO}} = 1$, and the band mass $m_b = 1$,

$$\hat{H} = \frac{\hat{\mathbf{p}}^2}{2} + \sum_{\mathbf{q}} \left(\hat{a}^+_{\mathbf{q}} \hat{a}_{\mathbf{q}} + \frac{1}{2} \right) + \frac{1}{\sqrt{V}} \sum_{\mathbf{q}} \frac{\sqrt{2\sqrt{2}\pi\alpha}}{q} (\hat{a}_{\mathbf{q}} + \hat{a}^+_{-\mathbf{q}}) e^{i\mathbf{q}\cdot\hat{\mathbf{r}}}, \tag{1}$$

where $\hat{\mathbf{r}}$ is the position operator of the electron and $\hat{\mathbf{p}}$ is its momentum operator; $\hat{a}^\dagger_{\mathbf{q}}$ and $\hat{a}_{\mathbf{q}}$ are, respectively, the creation and annihilation operators for LO phonons of wave vector $\mathbf{q}$. The electron-phonon coupling strength is described by the Fröhlich coupling constant α. As this Hamiltonian is quadratic in the phonon degrees of freedom, they can be integrated out analytically in the path-integral approach. The remaining electron degree of freedom is described via an action functional where the effects of electron-phonon interaction are contained in an influence phase $\Phi[\mathbf{r}_e(\tau)]$ [22]:

$$S[\mathbf{r}_e(\tau)] = \frac{1}{2} \int_0^\beta \dot{\mathbf{r}}_e^2(\tau) d\tau - \Phi[\mathbf{r}_e(\tau)]. \tag{2}$$

Here, $\mathbf{r}_e(\tau)$ is the path of the electron, expressed in imaginary time so as to obtain the Euclidean action, and $\beta = 1/(k_B T)$ with T the temperature. The influence phase corresponding to (1) depends on the difference in electron position at different times, resulting in a retarded action functional. In the path-integral formalism, thermodynamic potentials (such as the free energy) are calculated via the partition sum, which in turn is written as a sum over all possible paths $\mathbf{r}_e(\tau)$ of the electron that start and end in the same point, weighted by the exponent of the action.

Feynman's original variational method considers a *quadratic* trial action $S_{\mathrm{quad}}[\mathbf{r}_e(\tau), \mathbf{r}_f(\tau)]$ where the phonon degrees of freedom are replaced a a fictitious particle with coordinate $\mathbf{r}_f(\tau)$, interacting with the electron through a harmonic potential. Feynman restricted his trial action to a quadratic action, since only for this case can one calculate the influence phase analytically.

Using the Feynman variational approach with the Gaussian trial action, excellent results are obtained for the polaron ground-state energy, free energy, and the effective mass. Moreover, this approach has been effectively used to derive the DSG all-coupling theory for the polaron optical conductivity

(see Ref. [20]). However, as mentioned in Sec. I, the DSG and DQMC results contradict each other in the range of large α. The most probable source of this contradiction is the Gaussian form of the trial action used in the DSG theory. Indeed, the model system contains only a single frequency, leading to unphysically sharp peaks in the spectrum, subject to thermal broadening only [25,26]. Extensions to the formalism [18] have tried to overcome this problem by including an *ad hoc* broadening of the energy level, chosen in such as way as to comply with the sum rules. Remarkable success in the problem of the polaron optical response has been achieved in a recent work [27], where the all-coupling polaron optical conductivity is calculated using the general quadratic trial action instead of the Feynman model with a single fictitious particle. The resulting optical conductivity is in good agreement with DQMC results [13] in the weak- and intermediate-coupling regimes and is qualitatively in line with DQMC even at extremely strong coupling, resolving the issue of the linewidth in the FHIP approach. However, there is a quantitative difference between the results of [27] and DQMC in the strong-coupling regime, which is overcome in the present work.

In the literature, there are attempts to reformulate the Feynman variational approach, avoiding retarded trial actions. For example, Cataudella *et al.* [28] introduce an extended action which contains the coordinates of the electron, the fictitious particle, and the phonons. This action, however, is not exactly equivalent to the action of the electron-phonon system, and hence the results obtained in [28] need verification. In Ref. [29], we introduced an extended action/Hamiltonian for an electron-phonon system and reformulated the Feynman variational method in the Hamiltonian representation. This method leads to the same result as the Feynman variational approach. However, the method of Ref. [29] reproduces the strong-coupling limit for the polaron energy only when using a Gaussian trial action.

In the current work, we propose to extend the Feynman variational approach to trial systems with nonparabolic interactions between an electron and a fictitious particle. The difficulty with using non-Gaussian trial actions is that the path integrals with the influence phase can only be computed analytically for quadratic action functionals. However, quantum-statistical expectation values (such as the one in the Jensen-Feynman inequality) can be calculated for nonquadratic model systems by other means, in particular if the spectrum of eigenvalues and eigenfunctions can be found. So, what we propose is *to focus on keeping the influence phase for a quadratic model system in the expressions, while at the same time allowing for non-Gaussian potentials for the expectation values*.

The present variational method uses the following identical transformation as a starting point. Let us equivalently rewrite the partition function of the true electron-phonon system,

$$\mathcal{Z} = \int \mathcal{D}\mathbf{r}_e e^{-S[\mathbf{r}_e(\tau)]}, \tag{3}$$

as the extended path integral,

$$\mathcal{Z} = \frac{1}{\mathcal{Z}_f}\int \mathcal{D}\mathbf{r}_e \exp\{\Phi[\mathbf{r}_e(\tau)] - \Phi_{\rm quad}[\mathbf{r}_e(\tau)]\}\int \mathcal{D}\mathbf{r}_f \times \exp\left\{-\int_0^\beta \left[\frac{m\dot{\mathbf{r}}_e^2}{2} + \frac{m_f\dot{\mathbf{r}}_f^2}{2} + U_{\rm quad}(\mathbf{r}_f - \mathbf{r}_e)\right]d\tau\right\}, \tag{4}$$

with the partition function Z_f for a fictitious particle, and with the mass m_f in a harmonic potential $U_{\rm quad}(\mathbf{r}_f) = m_f^2\omega^2 r_f^2/2$. Indeed, performing the path integration for the fictitious particle cancels $\Phi_{\rm quad}[\mathbf{r}_e(\tau)]$ as well as the factor Z_f, and leaves the kinetic-energy contribution, restoring the action function of the true electron-phonon system. Hence, (3) and (4) are equivalent. The usefulness of the above transformation lies in the fact that (4) can be interpreted as an expectation value with respect to the model system. This identity transformation is being used here in the polaron problem.

In order to demonstrate the effectiveness of the transformation (4), consider a nonquadratic variational trial action,

$$S_{\rm var}[\mathbf{r}_e(\tau),\mathbf{r}_f(\tau)] = \int_0^\beta \left[\frac{m\dot{\mathbf{r}}_e^2}{2} + \frac{m_f\dot{\mathbf{r}}_f^2}{2} + U(\mathbf{r}_f - \mathbf{r}_e)\right]d\tau, \tag{5}$$

with a general potential U. We can rewrite (4) to the partition function,

$$\mathcal{Z} = \frac{\mathcal{Z}_{\rm var}}{\mathcal{Z}_f}\left\langle \exp\left\{\Phi[\mathbf{r}_e(\tau)] - \Phi_{\rm quad}[\mathbf{r}_e(\tau)] - \int_0^\beta [U_{\rm quad}(\mathbf{r}_f - \mathbf{r}_e) - U(\mathbf{r}_f - \mathbf{r}_e)]d\tau\right\}\right\rangle_{\rm var}, \tag{6}$$

where $Z_{\rm var}$ is the partition function for a trial system with the action $S_{\rm var}$. With $Z_{\rm var}/Z_f = e^{-\beta F_{\rm var}}$ and using the Jensen-Feynman variational inequality, we arrive at

$$F \leqslant F_{\rm var} + \frac{1}{\beta}\langle\Phi_{\rm quad}[\mathbf{r}_e(\tau)] - \Phi[\mathbf{r}_e(\tau)]\rangle_{\rm var} + \langle U_{\rm quad}(\mathbf{r}_f - \mathbf{r}_e) - U(\mathbf{r}_f - \mathbf{r}_e)\rangle_{\rm var.} \tag{7}$$

When $U = U_{\rm quad}$, this restores the original Jensen-Feynman variational principle for the polaron [22].

Introducing a nonquadratic potential leads to two changes. First, there is an additional term corresponding to the expectation value of the difference between the chosen variational potential and the quadratic one. Second, the expectation values are to be calculated with respect to the chosen variational potential U rather than with respect to the quadratic potential. Thus the variational inequality (7) is a nontrivial extension of the Feynman-Jensen inequality.

It is important for the calculations that $S_{\rm var}$ is translation invariant but nonretarded action, so that all expressions in the variational functional (7) have the same form in both representations—path-integral and standard quantum mechanics. Apart from the parameters appearing in the trial action $S_{\rm var}$, the inequality (7) still contains variational parameters m_f and ω, inherited from the "auxiliary" quadratic action $S_{\rm quad}$ and appearing in $\Phi_{\rm quad}$ and $U_{\rm quad}(\mathbf{r}_f - \mathbf{r}_e)$.

A physically reasonable choice of the trial interaction potential $U(\rho)$ with $\rho = |\mathbf{r}_f - \mathbf{r}|$ is no longer restricted to a single frequency oscillator. According to Refs. [23,30], the self-consistent potential for an electron induced by the lattice polarization is parabolic near the bottom and Coulomb-like at large distances. Therefore, for the calculation of the optical conductivity, we choose a trial potential in the piecewise form,

TABLE I. Parameters used for the calculation of the polaron optical conductivity within the memory-function formalism.

α	μ	ω	v	r_0
1	0.1035	3.139	3.882	2.499
3	0.3080	5.570	7.860	1.018
5.25	0.5255	5.189	8.885	0.733
6.5	0.6209	4.938	9.483	0.653

stitching together a parabolic and a Coulomb-like potential,

$$U(\rho) = \begin{cases} -U_0 + \frac{1}{2}\mu v^2 \rho^2, & \rho \leqslant r_0 \\ -\frac{\alpha_0}{\rho}, & \rho > r_0, \end{cases} \tag{8}$$

with the following variational parameters: the reduced mass $\mu = mm_f/(m+m_f)$, the bottom energy U_0, the confinement frequency v, and the parameter α_0 characterizing the Coulomb-like potential. The number of independent variational parameters is reduced because we impose the boundary conditions for $U(\rho)$ to be continuous and smooth at $\rho = r_0$. This leads to the following relations:

$$U_0 = \tfrac{3}{2}\mu v^2 r_0^2, \quad \alpha_0 = \mu v^2 r_0^3. \tag{9}$$

Thus the independent parameters for the present model are μ, ω, v, r_0.

In Table I, we represent optimal variational parameters for several values of α corresponding to the spectra of the optical conductivity calculated below within the memory-function formalism. The frequency v is the analog of the first variational frequency parameter v of the Feynman model, and ω has some similarity with the second one, w. Figure 1 shows the trial potential corresponding to these parameters. As can be seen from the figure, the potential becomes gradually deeper when α increases. Also the radius r_0 separating the parabolic and Coulomb-like fits for $U(r)$ decreases with an increasing coupling strength.

Because of using an auxiliary parabolic potential, the extended Jensen-Feynman inequality (7), despite having more variational parameters, does not lead in general to a lower

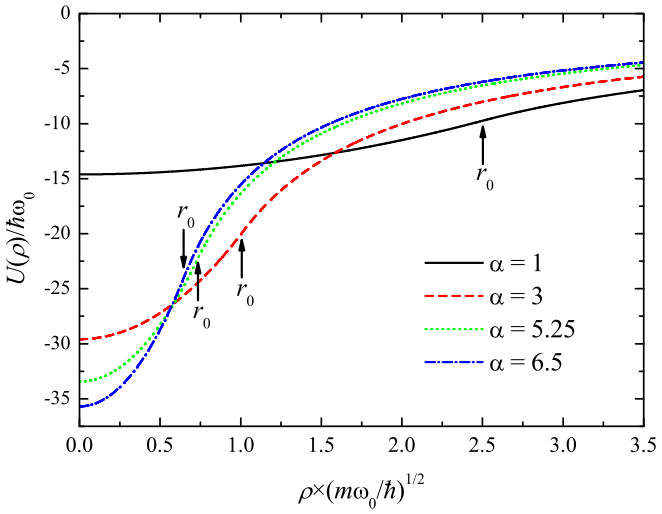

FIG. 1. Trial potential $U(\rho)$ calculated for parameters of the polaron model listed in Table I.

polaron free energy than the original Feynman result, except in the extremely strong-coupling regime where the present variational functional analytically tends (for $T = 0$) to the exact strong-coupling limit obtained by Miyake [30]. However, its advantage with respect to the original Feynman treatment is in calculating the optical conductivity. The spectrum of internal states of the model system with the chosen potential necessarily consists of an infinite number of nonequidistant energy levels with the energies $E_n < 0$ (counted from the potential energy at the infinity distance from the polaron) and a continuum of energies $E > 0$. Accounting for transitions between all of these levels, one must expect a significant broadening of the peak absorption.

The polaron optical conductivity is calculated following the scheme of Ref. [31], where the memory-function expression for the polaron optical conductivity is derived using the Mori-Zwanzig projection operator formalism [32]. We repeat the derivation up to formula (17) of Ref. [31], which is still formally exact. In the subsequent approximation, we extend the approach of Ref. [31], considering the density-density correlation function $\langle e^{i\mathbf{q}\cdot\mathbf{r}(t)} e^{-i\mathbf{q}\cdot\mathbf{r}(0)}\rangle_{\text{var}}$, where averaging is performed with the nonquadratic trial action/Hamiltonian. Note that these derivations in Ref. [31] and in the present work do not utilize the weak-coupling condition. As a result, the polaron optical conductivity takes the form

$$\sigma(\Omega) = \frac{e^2 n_0}{m_b} \frac{i}{\Omega - \chi(\Omega)/\Omega}, \tag{10}$$

where $n_0 = N/V$ is the carrier density. The memory function in the nonquadratic setting is given by

$$\chi(\Omega) = \frac{2}{3\hbar m_b} \int \frac{d\mathbf{q}}{(2\pi)^3} q^2 |V_{\mathbf{q}}|^2 \int_0^\infty dt e^{-\delta t} (e^{i\Omega t} - 1) \times \text{Im}\left\{ \frac{\cos[\omega_0(t + i\hbar\beta/2)]}{\sinh(\beta\hbar\omega_0/2)} \langle e^{i\mathbf{q}\cdot\mathbf{r}(t)} e^{-i\mathbf{q}\cdot\mathbf{r}(0)}\rangle_{\text{var}} \right\}, \tag{11}$$

where $\delta \to +0$, $\mathbf{r}(t)$ and $\mathbf{r}(0)$ are electron coordinate vectors in the Heisenberg representation with the Hamiltonian of the trial system, ω_0 is the LO phonon frequency, and the correlation function $\langle e^{i\mathbf{q}\cdot\mathbf{r}(t)} e^{-i\mathbf{q}\cdot\mathbf{r}(0)}\rangle_{\text{var}}$ is calculated with the quantum states of the trial Hamiltonian corresponding to S_{var}. In the quadratic setting, $\chi(\Omega)/\Omega$ exactly reproduces the function $\Sigma(\Omega)$ of Ref. [31]. Further on, we consider the case $T = 0$ and apply the formula following from (11),

$$\chi(\Omega) = \frac{1}{3\pi^2\hbar m_b} \lim_{\delta\to 0_+} \int_0^\infty dq |V_{\mathbf{q}}|^2 q^4 \int_0^\infty dt e^{-\delta t} (e^{i\Omega t} - 1) \times \text{Im}(e^{-i\omega_0 t} \langle e^{i\mathbf{q}\cdot\mathbf{r}(t)} e^{-i\mathbf{q}\cdot\mathbf{r}(0)}\rangle_{\text{var}}). \tag{12}$$

Rather than computing the correlation function $\langle e^{i\mathbf{q}\cdot\mathbf{r}(t)} e^{-i\mathbf{q}\cdot\mathbf{r}(0)}\rangle_{\text{var}}$ as a path integral, we choose to evaluate it in the equivalent Hamiltonian formalism. In this Hamiltonian framework, (12) is written as a sum over the eigenstates of the trial Hamiltonian for the electron and the fictitious particle interacting through the potential U,

$$\hat{H}_{\text{var}} = \frac{\hat{\mathbf{p}}^2}{2} + \frac{\hat{\mathbf{p}}_f^2}{2m_f} + U(\hat{\mathbf{r}}_f - \hat{\mathbf{r}}). \tag{13}$$

The quantum numbers for the Hamiltonian $\hat{H}_{\rm var}$ are the momentum $\mathbf{k}$, the quanta l,m related to angular momentum, and a nodal quantum number n for the relative-motion wave function. The quantum numbers l,n determine the energy $\varepsilon_{l,n}$ associated with the relative motion between electron and fictitious particle (including both the discrete and continuous parts of the energy spectrum). The eigenfunctions $|\psi_{\mathbf{k};l,n,m}\rangle$ of the trial Hamiltonian (13) are factorized as a product of a plane wave for the center-of-mass motion (with center-of-mass coordinate $\mathbf{R}$) and a wave function for the relative motion $|\varphi_{l,n,m}\rangle$ (with the coordinate vector $\boldsymbol{\rho}$ of the relative motion),

$$|\psi_{\mathbf{k};l,n,m}\rangle = \frac{1}{\sqrt{V}} e^{i\mathbf{k}\cdot\mathbf{R}} |\varphi_{l,n,m}\rangle, \tag{14}$$

$$|\varphi_{l,n,m}\rangle = \mathcal{R}_{l,n}(\rho) Y_{l,m}(\theta,\varphi). \tag{15}$$

The density-density correlation function at $T = 0$ is therefore the average with the ground state of the trial system, which can be expanded in the basis of eigenfunctions $|\psi_{\mathbf{k};l,n,m}\rangle$:

$$\begin{aligned}
&\langle e^{i\mathbf{q}\cdot\mathbf{r}(t)} e^{-i\mathbf{q}\cdot\mathbf{r}(0)}\rangle_{\rm var} \\
&\quad = \langle \psi_{\mathbf{0};0,0,0}| e^{\frac{i}{\hbar}\hat{H}_{\rm var} t} e^{i\mathbf{q}\cdot\mathbf{r}} e^{-\frac{i}{\hbar}\hat{H}_{\rm var} t} e^{-i\mathbf{q}\cdot\mathbf{r}} |\psi_{\mathbf{0};0,0,0}\rangle \\
&\quad = \sum_{\mathbf{k};l,n,m} e^{i\frac{t}{\hbar}(\varepsilon_{0,0}-\varepsilon_{l,n}-\frac{\hbar^2\mathbf{k}^2}{2M})} |\langle \psi_{\mathbf{0};0,0,0}| e^{i\mathbf{q}\cdot\mathbf{r}} |\psi_{\mathbf{k};l,n,m}\rangle|^2,
\end{aligned} \tag{16}$$

where $M = 1 + m_f$ is the total mass of the trial system. Further on, the Feynman units are used, where $\hbar = 1$, $\omega_0 = 1$, and the band mass $m_b = 1$. In these units, the squared modulus $|V_{\mathbf{q}}|^2$ is

$$|V_{\mathbf{q}}|^2 = \frac{2\sqrt{2}\pi\alpha}{q^2}.$$

When substituting (16) into the memory function, we arrive at the result

$$\begin{aligned}
\chi(\Omega) = \frac{2\sqrt{2}\alpha}{3\pi} \int_0^\infty dq q^2 \sum_{\mathbf{k};l,n,m} |\langle \psi_{\mathbf{0};0,0,0}| e^{i\mathbf{q}\cdot\mathbf{r}} |\psi_{\mathbf{k};l,n,m}\rangle|^2 \\
\times \int_0^\infty dt e^{-\delta t} (e^{i\Omega t} - 1) \,\mathrm{Im}(e^{-it(\varepsilon_{l,n}-\varepsilon_{0,0}+\frac{\mathbf{k}^2}{2M}+1)}).
\end{aligned} \tag{17}$$

Using analytic summations as described in the Appendix and the integration over time, the memory function takes the form

$$\begin{aligned}
\chi(\Omega) = \frac{\sqrt{2}\alpha}{3\pi} \int_0^\infty dq q^2 \sum_{l,n} (2l+1) S_q^2(0,0|l|l,n) \\
\times \left(\frac{1}{\Omega - \Omega_{q,l,n} + i\delta} - \frac{1}{\Omega + \Omega_{q,l,n} + i\delta} + \frac{2}{\Omega_{q,l,n}} \right), \\
\delta \to +0,
\end{aligned} \tag{18}$$

with the transition frequency for transitions between the ground and excited states of the trial system accompanied by an emission of a phonon,

$$\Omega_{q,l,n} \equiv \frac{q^2}{2M} + \varepsilon_{l,n} - \varepsilon_{0,0} + 1, \tag{19}$$

and the matrix element with radial wave functions for the trial system $S_q(l,n|l''|l',n')$ determined by (A6).

The limiting transition $\delta \to +0$ in (18) is performed analytically using the relation $\lim_{\delta\to+0}(x+i\delta)^{-1} = \mathcal{P}/x - i\pi\delta(x)$, where $\mathcal{P}/x$ is the Cauchy principal value and $\delta(x)$ is the delta function. This explicitly separates the real and imaginary parts of the memory function and eliminates the integration over q for the imaginary part. The obtained expressions are then used for the numerical calculation of the polaron optical conductivity within the extended memory-function formalism.

B. Nonadiabatic strong-coupling expansion

Next, we describe the strong-coupling approach and its extension beyond the adiabatic approximation, denoted below as the *nonadiabatic SCE*. Here, the goal is to take nonadiabatic transitions between different excited levels of a polaron into account in the formalism. The notations in this section are the same as in Ref. [19]. The polaron optical conductivity in the strong-coupling regime is represented by the Kubo formula,

$$\mathrm{Re}\,\sigma(\Omega) = \frac{\Omega}{2} \int_{-\infty}^{\infty} e^{i\Omega t} f_{zz}(t) dt, \tag{20}$$

with the dipole-dipole correlation function

$$\begin{aligned}
f_{zz}(t) = \sum_{n,l,m,\, n',l',m',\, n'',l'',m''} \langle \psi_{n,l,m}|\hat{z}|\psi_{n'',l'',m''}\rangle \langle \psi_{n',l',m'}|\hat{z}|\psi_0\rangle \\
\times \langle 0_{\rm ph}|\langle \psi_0| e^{it\hat{H}'} |\psi_{n,l,m}\rangle \langle \psi_{n'',l'',m''}| e^{-it\hat{H}'} \\
\times |\psi_{n',l',m'}\rangle |0_{\rm ph}\rangle,
\end{aligned} \tag{21}$$

where $|\psi_{n,l,m}\rangle$ are the polaron states as obtained within the strong-coupling ansatz in Ref. [19]. The transformed Hamiltonian $\hat{H}'$ of the electron-phonon system after the strong-coupling unitary transformation [19] takes the form

$$\hat{H}' = \hat{H}'_0 + \hat{W}, \tag{22}$$

with the terms

$$\hat{H}'_0 = \frac{\hat{\mathbf{p}}^2}{2} + \sum_{\mathbf{q}} |f_{\mathbf{q}}|^2 + V_a(\hat{\mathbf{r}}) + \sum_{\mathbf{q}} \left(\hat{b}^+_{\mathbf{q}} \hat{b}_{\mathbf{q}} + \frac{1}{2} \right), \tag{23}$$

$$\hat{W} = \sum_{\mathbf{q}} (\hat{w}_{\mathbf{q}} \hat{b}_{\mathbf{q}} + \hat{w}^*_{\mathbf{q}} \hat{b}^+_{\mathbf{q}}). \tag{24}$$

Here, $w_{\mathbf{q}}$ are the amplitudes of the renormalized electron-phonon interaction,

$$\hat{w}_{\mathbf{q}} = \frac{\sqrt{2\sqrt{2}\pi\alpha}}{q\sqrt{V}} (e^{i\mathbf{q}\cdot\hat{\mathbf{r}}} - \rho_{\mathbf{q},0}), \tag{25}$$

where $\rho_{\mathbf{q},0}$ is the expectation value of the operator $e^{i\mathbf{q}\cdot\hat{\mathbf{r}}}$ with the trial electron wave function $|\psi_0\rangle$,

$$\rho_{\mathbf{q},0} = \langle \psi_0| e^{i\mathbf{q}\cdot\hat{\mathbf{r}}} |\psi_0\rangle, \tag{26}$$

and $V_a(\hat{\mathbf{r}})$ is the self-consistent potential energy for the electron,

$$V_a(\hat{\mathbf{r}}) = -\sum_{\mathbf{q}} \frac{4\sqrt{2}\pi\alpha}{q^2 V} \rho_{-\mathbf{q},0} e^{i\mathbf{q}\cdot\hat{\mathbf{r}}}. \tag{27}$$

The eigenstates of the Hamiltonian $\hat{H}'_0$ are the products of the electron wave functions and those of the phonon vacuum

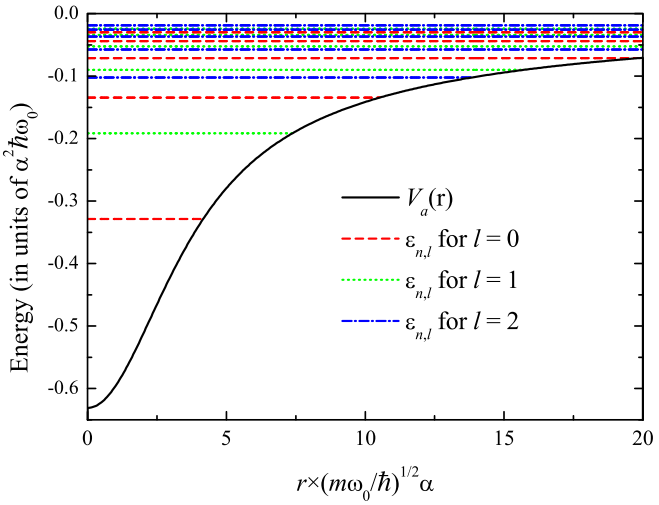

FIG. 2. Self-consistent potential $V_a(r)$ determined by (27) and energy levels for a polaron in the strong-coupling regime at $\alpha = 15$.

$|\psi_{n,l,m}\rangle|0_{\rm ph}\rangle$. The dipole-dipole correlation function $f_{zz}(t)$ given by (21) is simplified within the adiabatic approximation *for the ground state* and using the selection rules for the dipole transition matrix elements and the symmetry properties of the polaron Hamiltonian, as in Ref. [19]. The correlation function, using the interaction representation, takes the form

$$f_{zz}(t) = \sum_{n',n} \langle\psi_0|\hat{z}|\psi_{n,1,0}\rangle\langle\psi_{n',1,0}|\hat{z}|\psi_0\rangle e^{-i\Omega_{n,0}t} \times \langle\psi_{n,1,0}|\langle 0_{\rm ph}|T\exp\left[-i\int_0^t ds\,\hat{W}(s)\right]|0_{\rm ph}\rangle|\psi_{n',1,0}\rangle, \tag{28}$$

with the Franck-Condon (FC) transition frequency

$$\Omega_{n,0} \equiv \varepsilon_{n,1} - \varepsilon_{1,0},$$

and the interaction Hamiltonian in the interaction representation,

$$\hat{W}(s) = e^{i\hat{H}'s}\hat{W}e^{-i\hat{H}'s}.$$

As found in early works on the strong-coupling Fröhlich polaron (see, for review, Refs. [23,33]), the energy differences between different excited FC states for a strong-coupling polaron are much smaller than the energy difference between the ground and lowest excited FC state. For illustration, the self-consistent potential for the electron in the strong-coupling approximation $V_a(r)$ given by (27) and energy levels for an electron in this potential have been plotted for a polaron in the strong-coupling regime in Fig. 2. In the strong-coupling limit, the scaling invariance appears for energies, which are proportional to α^2, and for the length scale, which decreases in the strong-coupling regime as α^{-1}. Therefore, for sufficiently strong couplings, the energy diagrams plotted in units $(E/\alpha^2,\alpha r)$ depend only very slightly on α, tending to an α-independent picture when $\alpha \to \infty$. Thus we restricted the strong-coupling energy diagrams to one chosen α, e.g., here $\alpha = 15$. As can be seen from the figure, the difference $\varepsilon_{1,1} - \varepsilon_{1,0}$ is indeed large with respect to differences between excited levels. Therefore, here we keep the adiabatic approximation for the ground state and, consequently, for the transition between the ground and excited states. On the contrary, the adiabatic approximation for the transitions between *different excited states* is *not* applied in (28), as distinct from the calculation in Ref. [19].

The matrix elements for the dipole transitions from the ground state to excited states other than $|\psi_{1,1,0}\rangle$ (i.e., $\langle\psi_0|z|\psi_{n,1,0}\rangle$ with $n \neq 1$) have small relative oscillator strengths with respect to $\langle\psi_0|z|\psi_{1,1,0}\rangle$ (of the order of $\sim 10^{-2}$). Therefore further on we consider the next-to-leading-order nonadiabatic corrections for the contribution to (28) with $n = n' = 1$ and the adiabatic expression for the contribution with other (n,n'). In other words, for $n = n' = 1$, the treatment will account for nonadiabatic effects, while for other $n,n' \neq 1$, we apply the adiabatic approximation to (28). Consequently, the terms with $n' \neq n$, which are beyond this adiabatic approximation, are neglected in the next expression,

$$f_{zz}(t) = \sum_n |\langle\psi_0|\hat{z}|\psi_{n,1,0}\rangle|^2 e^{-i\Omega_{n,0}t} \times \langle\psi_{n,1,0}|\langle 0_{\rm ph}|T\exp\left[-i\int_0^t ds\,\hat{W}(s)\right]|0_{\rm ph}\rangle|\psi_{n,1,0}\rangle, \tag{29}$$

where T is the time-ordering symbol. The exact averaging over the phonon variables is performed by the disentangling of the evolution operator (in analogy with [34]). As a result, we obtain the formula

$$f_{zz}(t) = \sum_n |\langle\psi_0|z|\psi_{n,1,0}\rangle|^2 e^{-i\Omega_{n,0}t}\langle\psi_{n,1,0}|T_e\exp(\hat{\Phi})|\psi_{n,1,0}\rangle, \tag{30}$$

with the "influence phase" (assuming $\hbar = 1$ and $\omega_0 = 1$)

$$\hat{\Phi} = -\int_0^t ds\int_0^s ds' e^{-i(s-s')}\sum_{\mathbf{q}}\hat{w}_{\mathbf{q}}(s)\hat{w}^+_{\mathbf{q}}(s'), \tag{31}$$

and T_e the time-ordering symbol with respect to the electron degrees of freedom. The correlation function (30) is the basis expression for further treatment.

The next approximation is the restriction to the leading-order semi-invariant expansion:

$$\langle\psi_{n,1,0}|T_e\exp(\hat{\Phi})|\psi_{n,1,0}\rangle \approx \exp\langle\psi_{n,1,0}|T_e(\hat{\Phi})|\psi_{n,1,0}\rangle. \tag{32}$$

As shown in Ref. [19], this approximation accounts for the static Jahn-Teller effect, and it works well because the dynamic Jahn-Teller effect appears to be very small. The influence phase is invariant under spatial rotations so that

$$\langle\psi_{n,1,0}|T_e(\hat{\Phi})|\psi_{n,1,0}\rangle = \langle\psi_{n,1,1}|T_e(\hat{\Phi})|\psi_{n,1,1}\rangle = \langle\psi_{n,1,-1}|T_e(\hat{\Phi})|\psi_{n,1,-1}\rangle.$$

Hence the correlation function (30) can be simplified to

$$f_{zz}(t) = \sum_n |\langle\psi_0|\hat{z}|\psi_{n,1,0}\rangle|^2 \exp\left(-i\Omega_{n,0}t - \frac{1}{3}\sum_{\mathbf{q}}\sum_{n',l',m',m} |\langle\psi_{n,1,m}|\hat{w}_{\mathbf{q}}|\psi_{n',l',m'}\rangle|^2 \frac{1 - i\omega_{n',l';n,1}t - e^{-i\omega_{n',l';n,1}t}}{\omega^2_{n',l';n,1}}\right), \tag{33}$$

with the notation

$$\omega_{n',l';n,1} \equiv 1 + \varepsilon_{n',l'} - \varepsilon_{n,1}. \tag{34}$$

In our previous treatments of the strong-coupling polaron optical conductivity, we neglected the matrix elements for $\hat{w}_{\mathbf{q}}$ between the electron energy levels with different energies that correspond to the adiabatic approximation.

As described above, the correlation function (28) goes beyond this approximation, taking into account the transitions between different excited states but still assuming that the adiabatic approximation holds for the transitions between the ground and excited states. The physical picture beyond this approximation consists in the fact that the ground state is far below other states. Therefore, to be consistent with the above reasoning, we can keep in (33) the matrix elements $\langle\psi_{n,1,m}|\hat{w}_{\mathbf{q}}|\psi_{n',l',m'}\rangle$ only with the excited states, neglecting those matrix elements which contain the ground state. To summarize, here we keep the adiabatic approximation for the ground state and, consequently, for the transition between the ground and excited states. On the contrary, the adiabatic approximation for the transitions between different excited states is not assumed in (28) and (33), as distinct from the calculation in Ref. [19].

Introducing parameters related to the extension of the Huang-Rhys factor used in Ref. [19],

$$S_{n',l;n,1} \equiv \frac{1}{3\omega^2_{n',l;n,1}}\sum_{\mathbf{q}}\sum_{m',m} |\langle\psi_{n,1,m}|\hat{w}_{\mathbf{q}}|\psi_{n',l,m'}\rangle|^2, \tag{35}$$

the correlation function is rewritten as follows:

$$f_{zz}(t) = \sum_n |\langle\psi_0|z|\psi_{n,1,0}\rangle|^2 \exp\left[-i\Omega_{n,0}t - \sum_{n',l} S_{n',l;n,1}\left(1 - i\omega_{n',l;n,1}t - e^{-i\omega_{n',l;n,1}t}\right)\right]. \tag{36}$$

The states $|\psi_{n',l,m'}\rangle$ can be subdivided into two groups: (1) the states $|\psi_{1,1,m'}\rangle$ with the energy level $\varepsilon_{1,1}$, and (2) the higher-energy states with $(n',l) \neq (1,1)$. The first group of states was already taken into account in our previous treatments and in Ref. [19]. Taking into account the second group of states provides the step beyond the adiabatic approximation—this is the focus of the present treatment. We denote the parameters corresponding to the adiabatic approximation by

$$S_n \equiv S_{n,1;n,1} \equiv \frac{1}{3}\sum_{\mathbf{q}}\sum_{m',m} |\langle\psi_{n,1,m}|\hat{w}_{\mathbf{q}}|\psi_{n,1,m'}\rangle|^2. \tag{37}$$

Correspondingly, the correlation function (36) is rewritten as

$$f_{zz}(t) = \sum_n |\langle\psi_0|z|\psi_{n,1,0}\rangle|^2 \exp\left[-i\Omega_{n,0}t - S_n(1 - it - e^{-it}) - \sum_{(n',l)\neq(n,1)} S_{n',l;n,1}(1 - i\omega_{n',l;n,1}t - e^{-i\omega_{n',l;n,1}t})\right]. \tag{38}$$

When performing the Taylor expansion of this correlation function in powers of $S_n$and $S_{n',l;n,1}$ and substituting it into (20), the spectrum of the optical conductivity will give us a set of δ-like peaks, similar to formula (2) of Ref. [18], which is a Poissonian distribution. For sufficiently large coupling strengths, it is relevant to consider an envelope of this distribution, which is obtained in the following way. In the strong-coupling regime, the phonon frequency is small with respect to the Franck-Condon frequency $\Omega_{1,0}$, which increases as $\Omega_{1,0} \propto \alpha^2$ at large α. Therefore, at a strong coupling, the range of convergence for the integral over time in (20) is of the order of $t \propto 1/\Omega_{1,0} \ll 1$. Consequently, at large α, we can expand the factor $(1 - it - e^{-it})$ in powers of t up to the second order,

$$1 - it - e^{-it} = \tfrac{1}{2}t^2 + O(t^3). \tag{39}$$

In the particular case when nonadiabatic terms are not taken into account, the expansion (39) provides a Gaussian envelope of the optical conductivity spectrum obtained in [18,19]. The other factor $(1 - i\omega_{n',l;n,1}t - e^{-i\omega_{n',l;n,1}t})$ should not be expanded in the same way because the frequencies $\omega_{n',l;n,1}$ $(n',l) \neq (1,1)$ also increase in the strong-coupling limit as α^2. Therefore, we keep the nonadiabatic contribution as is, without expansion. As a result, in the strong-coupling regime, we arrive at the correlation function,

$$f_{zz}(t) = \sum_n |\langle\psi_0|z|\psi_{n,1,0}\rangle|^2 \exp\left(-\delta S_n - i\tilde{\Omega}_{n,0}t - \frac{1}{2}S_n t^2 + \sum_{(n',l)\neq(n,1)} S_{n',l;n,1}e^{-i\omega_{n',l;n,1}t}\right), \tag{40}$$

with the parameters

$$\delta S_n \equiv \sum_{(n',l)\neq(1,1)} S_{n',l;n,1}, \tag{41}$$

$$\delta\Omega_n \equiv \sum_{(n',l)\neq(1,1)} S_{n',l;n,1}\omega_{n',l;n,1}, \tag{42}$$

$$\tilde{\Omega}_{n,0} \equiv \Omega_{n,0} - \delta\Omega_n. \tag{43}$$

The parameter δS_n plays the role of the Debye-Waller factor and ensure the fulfillment of the f-sum rule for the optical conductivity. The parameter $\delta\Omega_n$ is the shift of the Franck-Condon frequency to a lower value due to phonon-assisted transitions to higher-energy states. The exponent can be expanded, yielding a description in terms of multiphonon processes:

$$\exp\left(\sum_{(n',l)\neq(n,1)} S_{n',l;n,1}e^{-i\omega_{n',l;n,1}t}\right) = \sum_{\{p_{n',l}\geqslant 0\}}\left(\prod_{(n',l)\neq(n,1)}\frac{S_{n',l;n,1}^{p_{n',l;n,1}}}{p_{n',l;n,1}!}\right)e^{-i\sum_{n',l}p_{n',l;n,1}\omega_{n',l;n,1}t}, \tag{44}$$

where the sum $\sum_{\{p_{n',l}\}}$ is performed over all combinations $\{p_{n',l}\geqslant 0\}$.

With the expansion (44), the polaron optical conductivity takes the form

$$\mathrm{Re}\,\sigma(\Omega) = \Omega\sum_n |\langle\psi_0|z|\psi_{n,1,0}\rangle|^2 e^{-\delta S_n}\sqrt{\frac{\pi}{2S_n}}\sum_{\{p_{n',l;n,1}\geqslant 0\}}\left(\prod_{(n',l)\neq(n,1)}\frac{S_{n',l;n,1}^{p_{n',l;n,1}}}{p_{n',l;n,1}!}\right)\exp\left[-\frac{\left(\tilde{\Omega}_{n,0}+\sum_{n',l}p_{n',l;n,1}\omega_{n',l;n,1}-\Omega\right)^2}{2S_n}\right]. \tag{45}$$

In formula (45), the term where all $p_{n',l;n,1} = 0$ corresponds to the adiabatic approximation and exactly reproduces the result of Ref. [19]. The other terms represent the *nonadiabatic* contributions to $\mathrm{Re}\,\sigma(\Omega)$ and are correction terms to the previously found results.

III. RESULTS AND DISCUSSIONS

The polaron optical conductivity derived in the above section is in line with the physical understanding of the underlying processes for the polaron optical response, achieved in early works [20,35] and summarized in Ref. [36]. It is based on the concept of the polaron excitations of three types:

(i) relaxed excited states (RES) [35] for which the lattice polarization is adapted to the electronic distribution;

(ii) Franck-Condon states (FC) where the lattice polarization is "frozen," adapted to the polaron ground state; and

(iii) scattering states characterized by the presence of real phonons along with the polaron.

These polaron excitations are schematically shown in Fig. 3. The polaron RES can be formed when the electron-phonon coupling is strong enough, for $\alpha \gtrapprox 4.5$. At weak coupling, the polaron optical response at zero temperature is due to transitions from the polaron ground state to scattering states. In other words, the optical absorption spectrum of a weak-coupling polaron is determined by the absorption of radiation energy, which is reemitted in the form of LO phonons. At stronger couplings, the concept of the polaron relaxed excited states introduced in Ref. [35] becomes of key importance. In the range of sufficiently large α when the polaron RES are formed, the absorption of light by a polaron occurs through transitions from the ground state to RES, which can be accompanied by the emission of different numbers $n \geqslant 0$ of free phonons. These transitions contribute to the shape of a multiphonon optical absorption spectrum. At very large coupling, lattice relaxation processes become too slow and the Franck-Condon states determine the optical response.

We analyze polaron optical conductivity spectra both with the memory-function formalism and with the strong-coupling expansion, and compare these to the DQMC numerical data [13]. Within the framework of formalisms based on the memory function (MF), we compare the following theories:

(a) The original DSG method of Ref. [20], where the expectation value in (17) is calculated with respect to a Gaussian trial action. This will be denoted by MF-1 in the figures.

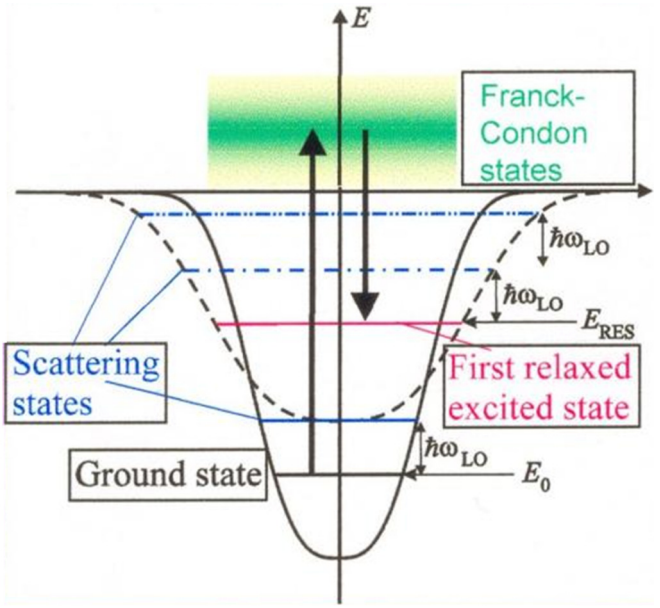

FIG. 3. Structure of the energy spectrum of a polaron at strong coupling, according to Refs. [35–37].

(b) The extended MF formalism of [18], where an *ad hoc* broadening with a strength determined from sum rules is included in (10). This will be denoted by MF-2.

(c) The current nonquadratic MF formalism, based on the extension of the Jensen-Feynman inequality introduced in this paper, denoted by MF-new.

Among the strong-coupling expansions (SCE), we distinguish the following:

(1) The strong-coupling result in the adiabatic approximation, as obtained in Ref. [18]. This will be denoted here by SCE-1.

(2) The adiabatic approximation of Ref. [19], which uses more accurate trial polaron states. This will be denoted by SCE-2.

(3) The current nonadiabatic strong-coupling expansion, denoted by SCE-new.

The subsequent figures show the results for increasing α. In Fig. 4, the optical conductivity is shown for small coupling, $\alpha = 1$, and for $\alpha = 3$,$\alpha = 5.25$, which correspond to the dynamic regime where the RES start to play a role. In this regime, analytic solutions are provided by the various memory-function formalisms listed above, and we compare them to DQMC numeric data [13]. At weak coupling $\alpha = 1$ [Fig. 4(a)], all of the approaches based on the memory function give results in agreement with DQMC. For $\alpha = 3$ [Fig. 4(b)], the current method gives a better fit to the DQMC result than the other two methods. For a stronger coupling $\alpha = 5.25$ [Fig. 4(c)], the MF-2 approach substantially improves the original result MF-1, but the optical conductivity spectrum calculated within the nonquadratic MF-new formalism lies closer to the DQMC data than either of the other two.

Figure 5 demonstrates the behavior of the polaron optical conductivity spectra in the intermediate-coupling regime, for $\alpha = 6.5$ and $\alpha = 7$. In this regime, the existing memory-function approaches (MF-1, MF-2) as well as the existing strong-coupling expansions (SCE-1, SCE-2) do not provide satisfactory results. The memory-function approach presented here and the strong-coupling expansion presented here are in much better agreement with the DQMC data.

This range of coupling parameters is where one would want to cross over from using a memory-function-based approach to a strong-coupling expansion. Whereas the existing methods do not allow one to bridge this gap at intermediate coupling, the extensions that we have proposed here are suited to implement such a crossover. The present memory-function approach with the nonparabolic trial action leads to a relatively small extension of the range of α where the polaron optical conductivity compares well with the DQMC data, namely from $\alpha \approx 4.5$ to $\alpha \approx 6.5$. For $\alpha \lessapprox 6.5$, the memory-function approach with the nonparabolic trial action provides a better agreement with DQMC than all other known approximations. Remarkably, the optical conductivity spectra as given by the nonquadratic MF formalism and the nonadiabatic SCE are both in better agreement with the Monte Carlo data than any of the preceding analytical methods. For $\alpha = 6.5$, the polaron optical conductivity calculated within nonquadratic MF formalism and the nonadiabatic SCE lie rather close to each other. We can conclude, therefore, that the ranges of validity of those two approximations overlap, despite the fact that these approximations are based on different assumptions.

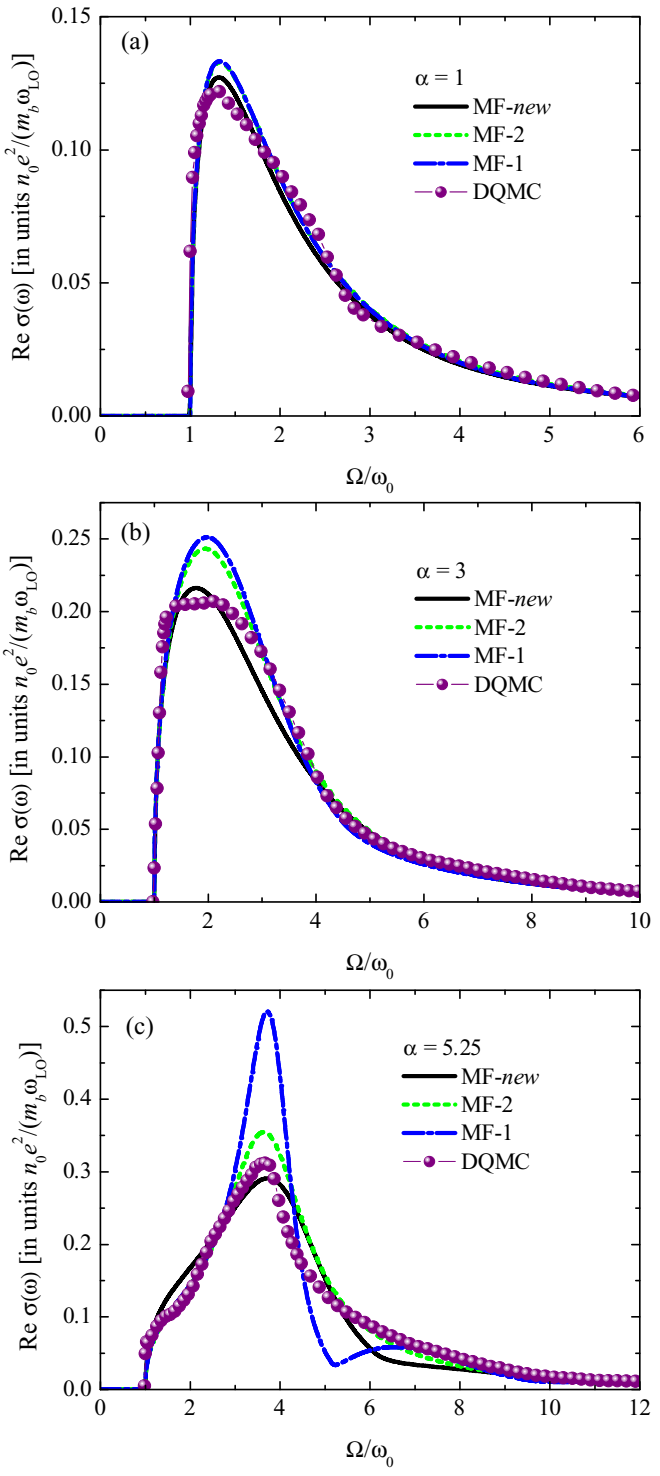

FIG. 4. Polaron optical conductivity calculated for (a) $\alpha = 1$, (b) $\alpha = 3$, and (c) $\alpha = 5.25$ within the present nonquadratic MF formalism (denoted in the figure as MF-new), compared with the polaron optical conductivity calculated within the extended memory-function formalism (MF-2) of Ref. [18], the results of the memory-function approach using the Feynman parabolic trial action [20] (MF-1), and the diagrammatic quantum Monte Carlo (DQMC) [13,18].

The maximum of the optical conductivity spectrum provided by the nonquadratic MF formalism for $\alpha = 6.5$ is

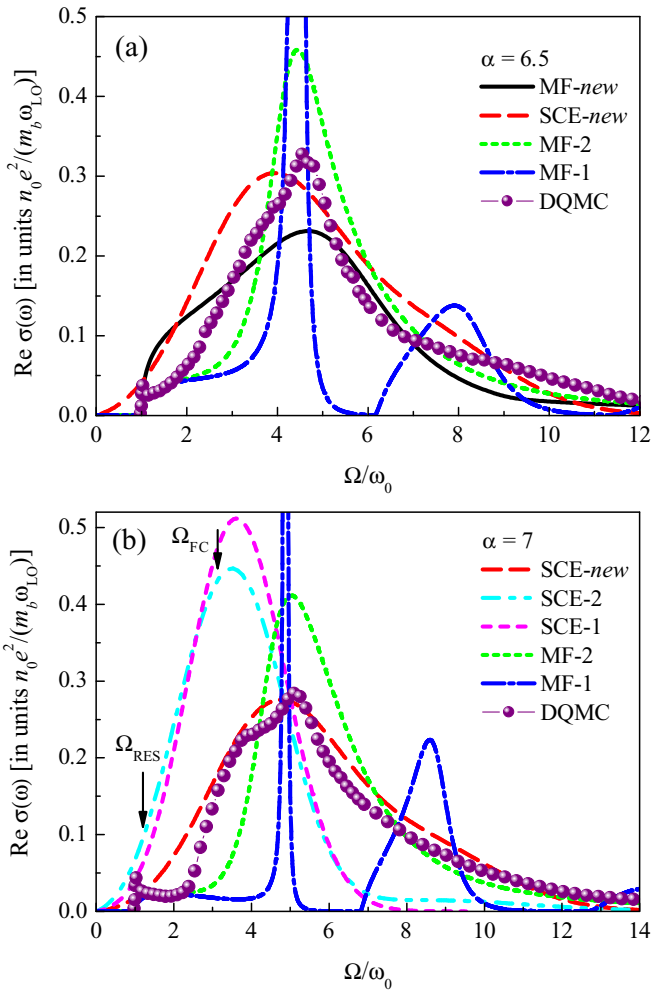

FIG. 5. Polaron optical conductivity calculated for (a) $\alpha = 6.5$ and (b) $\alpha = 7$ using different analytic approaches: the nonquadratic MF formalism (MF-new), the extended memory-function formalism of Ref. [18] (MF-2), the memory-function approach with the Feynman parabolic trial action [20] (MF-1), the nonadiabatic strong-coupling expansion (SCE-new), and the adiabatic strong-coupling expansions of Refs. [18,19] (SCE-1 and SCE-2). The results are compared to DQMC data of Refs. [13,18].

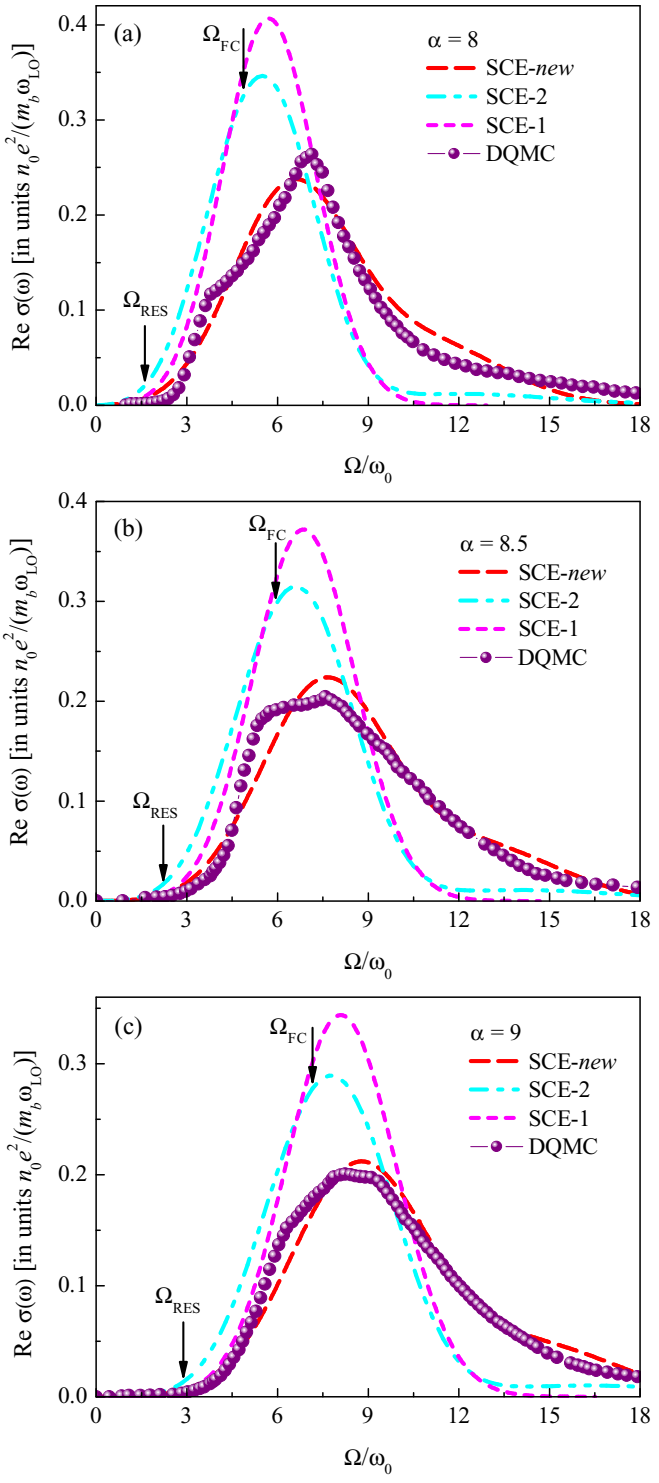

FIG. 6. Polaron optical conductivity calculated for (a) $\alpha = 8$, (b) $\alpha = 8.5$, and (c) $\alpha = 9$ within several analytic strong-coupling approaches and compared to the DQMC data of Refs. [13,18]. The notations are the same as in Fig. 5.

positioned at slightly higher frequency than that for the maximum of the optical conductivity obtained in the strong-coupling approximation with nonadiabatic corrections. They lie remarkably close to two features of the DQMC optical conductivity spectrum: the higher-frequency peak, which is the maximum of the spectrum, and the lower-frequency shoulder. The similar comparative behavior of the memory-function and strong-coupling results was noticed in Ref. [18], where it was suggested that these two features in the DQMC spectra can correspond physically to the dynamic (RES) and the Franck-Condon contributions. The present results are in line with that physical picture.

In Fig. 5(b), the arrows indicate the FC transition frequency for the transition to the first excited FC state $\Omega_{1,0} \equiv \Omega_{\rm FC}$ and the RES transition frequency $\Omega_{\rm RES}$ for a strong coupling polaron, as calculated in Ref. [35]. We can see that both the shape and the position of the maximum of the optical conductivity band obtained within the adiabatic approximation in Refs. [18,19] are rather far from those for the DQMC data. Taking into account nonadiabatic transitions drastically improves the agreement of the strong-coupling approximation with DQMC, even for $\alpha = 7$, which, strictly speaking, is

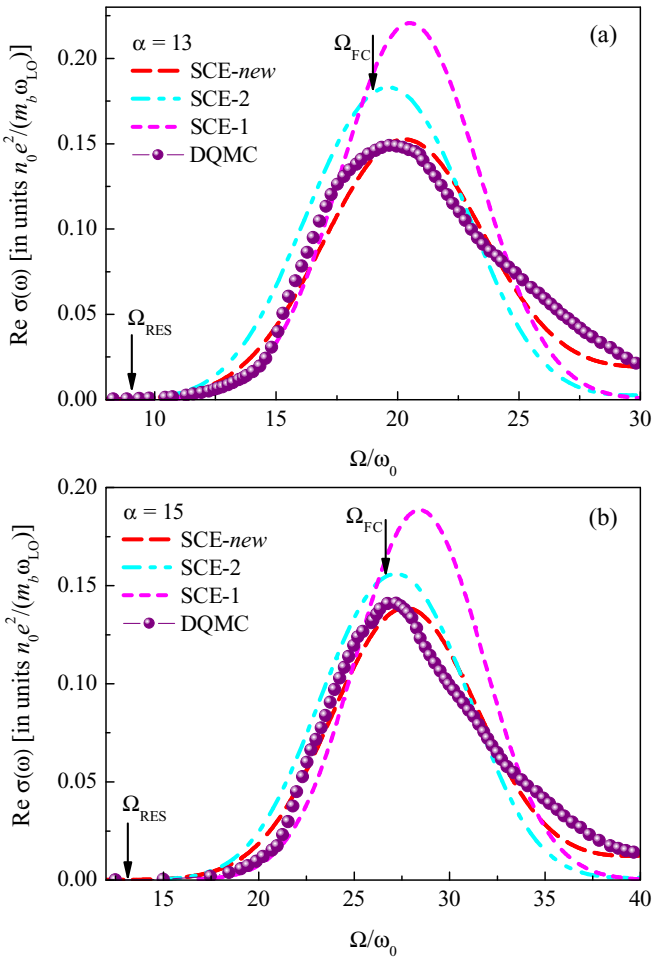

FIG. 7. Polaron optical conductivity in the extremely strong-coupling regime, for (a) $\alpha = 13$ and (b) $\alpha = 15$. The notations are the same as in Fig. 5.

not yet the strong-coupling regime. The value $\alpha = 7$ can be rather estimated as an intermediate coupling. However, even at this intermediate-coupling strength, the results of the present approach lie much closer to the DQMC data than those obtained within all other aforesaid analytic methods. Also a substantial improvement of the agreement between the strong-coupling expansion and DQMC is clearly expressed in Fig. 6, where the polaron optical conductivity spectra are shown for the strong-coupling regime for $\alpha = 8$ to $\alpha = 9$. For strong couplings, the nonadiabatic SCE accurately reproduces both the peak position and the overall shape of the DQMC spectra. Finally, we see that the results of the nonadiabatic SCE remain accurate also in the extremely strong-coupling regime, as shown in Fig. 7.

IV. CONCLUSIONS

In the present work, we have modified two basic analytic methods for the polaron optical conductivity in order to extend their ranges of applicability for the electron-phonon coupling constant in such a way that these ranges overlap. The memory-function formalism using a trial action for a model two-particle system has been extended to work with nonquadratic interaction potentials in the model system. This method combines the translation invariance of the trial system, which is one of the main advantages of the Feynman variational approach, with a more realistic interaction between the electron and the fictitious particle. This extension leads to a substantial improvement of the polaron optical conductivity for small- and intermediate-coupling strengths with respect to the preceding known versions of the memory-function approach.

The other method is the strong-coupling expansion, and we have extended it beyond the Franck-Condon adiabatic approximation by taking into account nonadiabatic transitions between different excited polaron states. As a result, the modified nonadiabatic strong-coupling expansion appears now to be in good agreement with the numerical DQMC data in a wide range of α, from intermediate-coupling strength to the strong-coupling limit. For the intermediate-coupling value $\alpha = 6.5$, the two methods that we propose, i.e., the nonquadratic MF formalism and the nonadiabatic SCE, result in optical conductivity spectra which are remarkably close to each other and to the DQMC results. Thus, both methods can be combined to provide all-coupling, accurate analytic results for the polaron optical absorption.

For larger α, the agreement between the results of the nonadiabatic SCE and DQMC becomes gradually better. At very strong coupling, even the preceding adiabatic SCE [19] is already sufficiently good, so that the improvement due to the nonadiabatic transitions, e.g., for $\alpha = 15$, is relatively small. However, for a slightly weaker coupling, e.g., for $\alpha = 9$, we can observe a drastically improved agreement with DQMC for the present nonadiabatic SCE as compared to the adiabatic approximation. We can conclude that at present, the strong-coupling approximation, taking into account nonadiabatic contributions, provides the best agreement with the DQMC results for $\alpha \gtrapprox 6.5$ compared to other known analytic approaches for the polaron optical conductivity. We find that the nonadiabatic transitions lead to a substantial change of the spectral shape with respect to the optical conductivity derived within the adiabatic approximation. The nonadiabatic effects are non-negligible in the whole range of the coupling strength, at least for $\alpha \leqslant 15$, available for DQMC.

As discussed in Ref. [33], at strong coupling the distances between different polaron energy levels rise as $\propto \alpha^2$, and hence the matrix elements of the electron-phonon interaction diminish. Thus the small parameter in the strong-coupling approximation for a polaron is $1/\alpha$. The contribution to the optical conductivity taking into account nonadiabatic transitions represent in fact the next-to-leading-order correction in powers of this small parameter. Consequently, this correction is more significant at weaker couplings, and is relatively small at strong coupling. The comparison of the calculated optical conductivity with DQMC confirms this prediction.

In summary, extending the MF and SCE formalisms leads to an overlapping of the areas of α where these two analytic methods are applicable. These analytic methods have been verified, appearing to be in good agreement with numeric DQMC data at all α available for DQMC. We therefore possess the analytic description of the polaron optical response which embraces the whole range of the coupling strength.

ACKNOWLEDGMENTS

We thank A. S. Mishchenko for valuable discussions and for the DQMC data for the polaron optical conductivity, and we thank V. Cataudella for the details of the EMFF method. Discussions with F. Brosens and D. Sels are gratefully acknowledged. This research has been supported by the Flemish Research Foundation (FWO-Vl), Projects No. G.0115.12N, No. G.0119.12N, No. G.0122.12N, and No. G.0429.15N, by the Scientific Research Network of the Flemish Research Foundation, Grant No. WO.033.09N, and by the Research Fund of the University of Antwerp.

APPENDIX: ANALYTIC SUMMATIONS

The matrix element in (17) is a particular case of the product of two matrix elements:

$$\langle\psi_{\mathbf{k};l,n,m}|e^{i\mathbf{q}\cdot\mathbf{r}}|\psi_{\mathbf{k}';l',n',m'}\rangle = \frac{1}{V}\langle e^{-i\mathbf{k}\mathbf{R}}|e^{i\mathbf{q}\cdot\mathbf{R}}|e^{i\mathbf{k}'\mathbf{R}}\rangle\langle\varphi_{l,n,m}|e^{i\mu\mathbf{q}\cdot\boldsymbol{\rho}}|\varphi_{l',n',m'}\rangle, \quad \text{(A1)}$$

where μ is the reduced mass of the trial system. The first matrix element is

$$\frac{1}{V}\langle e^{-i\mathbf{k}\mathbf{R}}|e^{i\mathbf{q}\cdot\mathbf{R}}|e^{i\mathbf{k}'\mathbf{R}}\rangle = \delta_{\mathbf{k}',\mathbf{k}-\mathbf{q}}. \quad \text{(A2)}$$

This eliminates the integration over the final electron momentum $\mathbf{k}'$ and reduces the memory function to the expression

$$\chi(\Omega) = \frac{2\sqrt{2}\alpha}{3\pi}\int_0^\infty dqq^2\sum_{l',n',m'}|\langle\varphi_{0,0,0}|e^{i\mu\mathbf{q}\cdot\boldsymbol{\rho}}|\varphi_{l',n',m'}\rangle|^2 \times\int_0^\infty dte^{-\delta t}(e^{i\Omega t}-1)\,\mathrm{Im}\left(e^{-it(\frac{q^2}{2M}+\varepsilon_{l',n'}-\varepsilon_{0,0}+1)}\right). \quad \text{(A3)}$$

For a more general expression $|\langle\varphi_{l,n,m}|e^{i\mu\mathbf{q}\cdot\boldsymbol{\rho}}|\varphi_{l',n',m'}\rangle|^2$, the summation over m and m' is performed explicitly:

$$\sum_{m,m'}|\langle\varphi_{l,n,m}|e^{i\mu\mathbf{q}\cdot\boldsymbol{\rho}}|\varphi_{l',n',m'}\rangle|^2 = \frac{(2l+1)(2l'+1)}{2}\int_0^\infty\rho^2d\rho\int_0^\infty(\rho')^2d\rho' \times\mathcal{R}_{l,n}(\rho)\mathcal{R}_{l',n'}(\rho)\mathcal{R}_{l,n}(\rho')\mathcal{R}_{l',n'}(\rho') \times\int_0^{2\pi}\frac{\sin(\mu q|\boldsymbol{\rho}-\boldsymbol{\rho}'|)}{\mu q|\boldsymbol{\rho}-\boldsymbol{\rho}'|}P_l(\cos\theta)P_{l'}(\cos\theta)\sin\theta d\theta. \quad \text{(A4)}$$

The modulus $|\boldsymbol{\rho}-\boldsymbol{\rho}'|$ is expressed as

$$|\boldsymbol{\rho}-\boldsymbol{\rho}'| = \sqrt{\rho^2+(\rho')^2-2\rho\rho'\cos\theta}. \quad \text{(A5)}$$

Hence we can use the expansion of $\frac{\sin(\mu q|\boldsymbol{\rho}-\boldsymbol{\rho}'|)}{\mu q|\boldsymbol{\rho}-\boldsymbol{\rho}'|}$ through the Legendre polynomials $P_l(z)$ and spherical Bessel functions $j_l(z)$,

$$\frac{\sin(\mu q|\boldsymbol{\rho}-\boldsymbol{\rho}'|)}{\mu q|\boldsymbol{\rho}-\boldsymbol{\rho}'|} = \sum_{l''=0}^\infty(2l''+1)j_{l''}(\mu q\rho)j_{l''}(\mu q\rho')P_{l''}(\cos\theta).$$

The integral of the product of three Legendre polynomials is expressed through the $3j$ symbol,

$$\int_0^{2\pi}P_{l''}(\cos\theta)P_l(\cos\theta)P_{l'}(\cos\theta)\sin\theta d\theta = 2\begin{pmatrix}l & l' & l''\\ 0 & 0 & 0\end{pmatrix}^2.$$

Therefore, we find that

$$\sum_{m,m'}|\langle\varphi_{l,n,m}|e^{i\mu\mathbf{q}\cdot\boldsymbol{\rho}}|\varphi_{l',n',m'}\rangle|^2 = \sum_{l''=0}^\infty(2l+1)(2l'+1)(2l''+1) \times\begin{pmatrix}l & l' & l''\\ 0 & 0 & 0\end{pmatrix}^2 S_q^2(l,n|l''|l',n'),$$

where $S_q(l,n|l''|l',n')$ is the matrix element with radial wave functions for the trial system,

$$S_q(l,n|l''|l',n') \equiv \int_0^\infty\mathcal{R}_{l,n}(\rho)\mathcal{R}_{l',n'}(\rho)j_{l''}(\mu q\rho)\rho^2d\rho. \quad \text{(A6)}$$

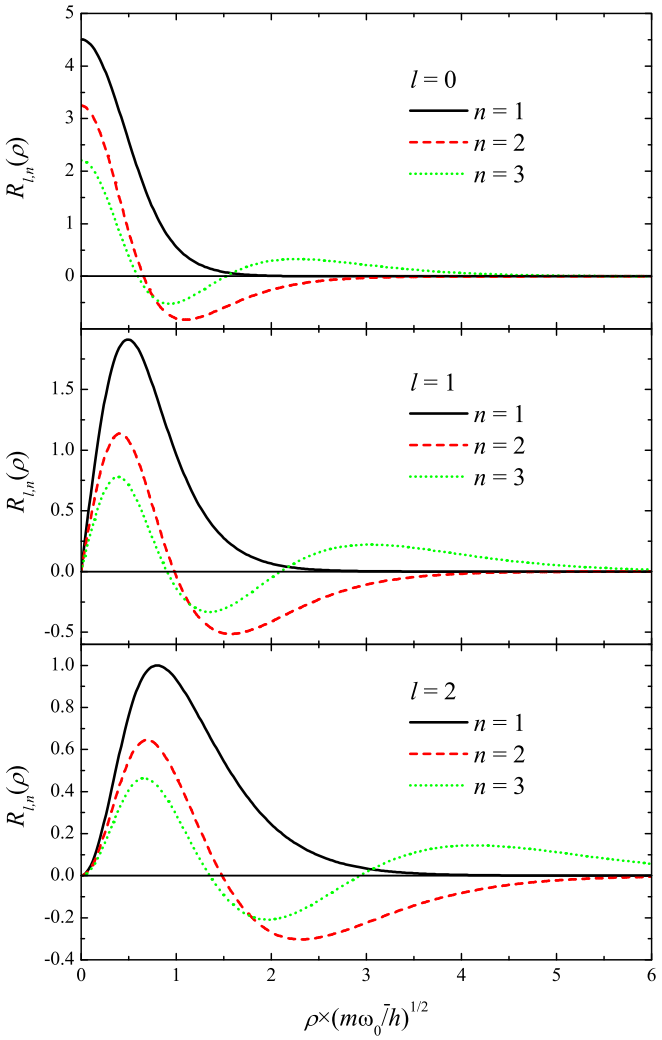

FIG. 8. Radial wave functions $\mathcal{R}_{l,n}(\rho)$ calculated for several values of the quantum numbers l,n.

For $l = 0$, the result of the summation over intermediate states is reduced to the formula

$$\sum_{m'} |\langle \varphi_{0,n,0}|e^{i\mu\mathbf{q}\cdot\boldsymbol{\rho}}|\varphi_{l',n',m'}\rangle|^2 = (2l'+1)S_q^2(0,0|l'|l',n'), \quad \text{(A7)}$$

which is used in our calculations.

Figure 8 shows radial wave functions $\mathcal{R}_{l,n}(\rho)$ entering the matrix elements. The wave functions are plotted for several lowest values of the quantum numbers l,n. The figure corresponds to the intermediate-coupling regime with $\alpha = 5.25$. These radial wave functions represent analytically exact solutions of the Schrödinger equation for a particle with the reduced mass μ in the trial potential $U(\rho)$ given by (8).

[1] L. D. Landau, Physikalische Zeitschrift der Sowjetunion **3**, 664 (1933) [English translation in *Collected Papers* (Gordon and Breach, New York, 1965), pp. 67–68].

[2] A. S. Alexandrov and J. T. Devreese, *Advances in Polaron Physics* (Springer, New York, 2009).

[3] R. von Helmolt, J. Wecker, B. Holzapfel, L. Schultz, and K. Samwer, Phys. Rev. Lett. **71**, 2331 (1993).

[4] H. Sirringhaus *et al.*, Nature (London) **401**, 685 (1999).

[5] M. Setvin, C. Franchini, X. Hao, M. Schmid, A. Janotti, M. Kaltak, C. G. Van de Walle, G. Kresse, and U. Diebold, Phys. Rev. Lett. **113**, 086402 (2014).

[6] X. Hao, Z. Wang, M. Schmid, U. Diebold, and C. Franchini, Phys. Rev. B **91**, 085204 (2015).

[7] T. Holstein, Ann. Phys. (NY) **8**, 325 (1959).

[8] J. Vlietinck, W. Casteels, K. Van Houcke, J. Tempere, J. Ryckebusch, and J. T. Devreese, New J. Phys. **17**, 033023 (2015).

[9] W. Meevasana, X. J. Zhou, B. Moritz, C.-C. Chen, R. H. He, S.-I. Fujimori, D. H. Lu, S.-K. Mo, R. G. Moore, F. Baumberger, T. P. Devereaux, D. van der Marel, N. Nagaosa, J. Zaanen, and Z.-X. Shen, New J. Phys. **12**, 023004 (2010).

[10] J. L. M. van Mechelen, D. van der Marel, C. Grimaldi, A. B. Kuzmenko, N. P. Armitage, N. Reyren, H. Hagemann, and I. I. Mazin, Phys. Rev. Lett. **100**, 226403 (2008).

[11] J. T. Devreese, S. N. Klimin, J. L. M. van Mechelen, and D. van der Marel, Phys. Rev. B **81**, 125119 (2010).

[12] A. S. Mishchenko, N. V. Prokof'ev, A. Sakamoto, and B. V. Svistunov, Phys. Rev. B **62**, 6317 (2000).

[13] A. S. Mishchenko, N. Nagaosa, N. V. Prokof'ev, A. Sakamoto, and B. V. Svistunov, Phys. Rev. Lett. **91**, 236401 (2003).

[14] G. L. Goodvin, A. S. Mishchenko, and M. Berciu, Phys. Rev. Lett. **107**, 076403 (2011).

[15] V. L. Gurevich, I. G. Lang, and Yu. A. Firsov, Fiz. Tverd. Tela **4**, 1252 (1962) [Sov. Phys. Solid State **4**, 918 (1962)].

[16] J. Devreese, W. Huybrechts, and L. Lemmens, Phys. Status Solidi B **48**, 77 (1971).

[17] B. E. Sernelius, Phys. Rev. B **48**, 7043 (1993).

[18] G. De Filippis, V. Cataudella, A. S. Mishchenko, C. A. Perroni, and J. T. Devreese, Phys. Rev. Lett. **96**, 136405 (2006).

[19] S. N. Klimin and J. T. Devreese, Phys. Rev. B **89**, 035201 (2014).

[20] J. Devreese, J. De Sitter, and M. Goovaerts, Phys. Rev. B **5**, 2367 (1972).

[21] R. P. Feynman, R. W. Hellwarth, C. K. Iddings, and P. M. Platzman, Phys. Rev. **127**, 1004 (1962).

[22] R. P. Feynman, Phys. Rev. **97**, 660 (1955).

[23] S. I. Pekar, *Untersuchungen über die Elektronentheorie der Kristalle* (Akademie-Verlag, Berlin, 1954).

[24] K. Huang and A. Rhys, Proc. R. Soc. London, Ser. A **204**, 406 (1950).

[25] D. Sels and F. Brosens, Phys. Rev. E **89**, 012124 (2014).

[26] D. Sels and F. Brosens, Phys. Rev. E **89**, 042110 (2014).

[27] D. Sels, arXiv:1605.04998.

[28] V. Cataudella, G. De Filippis, and C. A. Perroni, in *Polarons in Advanced Materials*, edited by A. S. Alexandrov, Springer Series in Materials Science, Vol. 103 (Springer, New York, 2007), pp. 149–189.

[29] S. N. Klimin and J. T. Devreese, Solid State Commun. **151**, 144 (2011).

[30] S. J. Miyake, J. Phys. Soc. Jpn. **38**, 181 (1975).

[31] F. M. Peeters and J. T. Devreese, Phys. Rev. B **28**, 6051 (1983).

[32] H. Mori, Prog. Theor. Phys., **33**, 423 (1965); **34**, 399 (1965).

[33] G. R. Allcock, in *Polarons and Excitons*, edited by C. G. Kuper and G. D. Whitfield (Oliver and Boyd, Edinburgh, 1963), pp. 45–70.

[34] R. P. Feynman, Phys. Rev. **84**, 108 (1951).

[35] E. Kartheuser and R. Evrard, and J. Devreese, Phys. Rev. Lett. **22**, 94 (1969).

[36] J. T. Devreese, in *Polarons in Ionic Crystals and Polar Semiconductors* (North-Holland, Amsterdam, 1972), pp. 83–159.

[37] J. T. Devreese, in *Lectures on the Physics of Highly Correlated Electron Systems* (AIP, Melville, 2003), pp. 3–56.